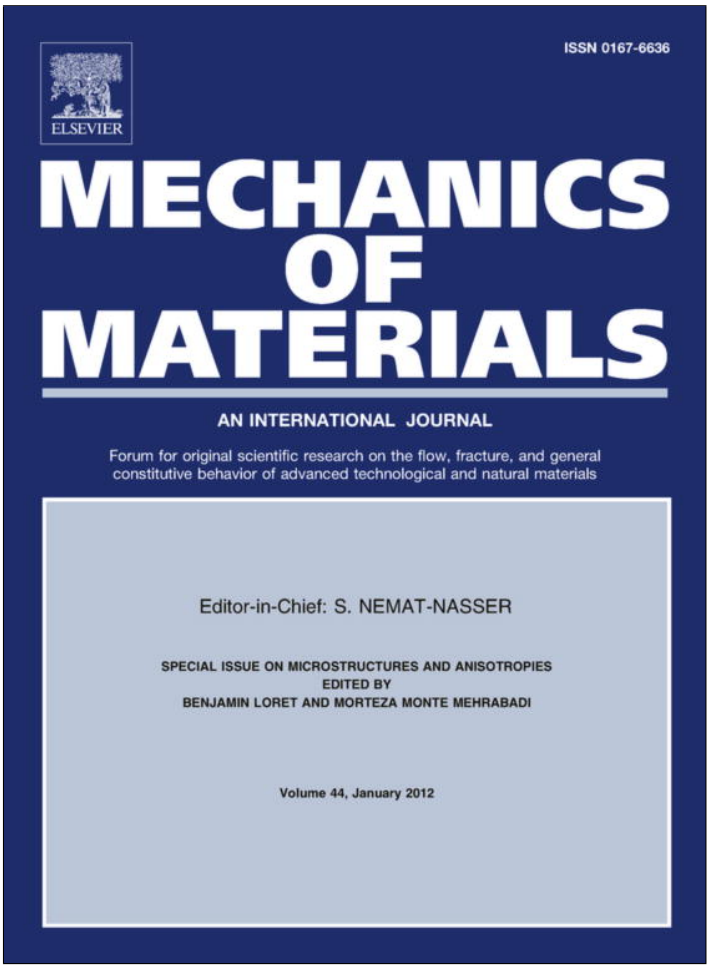

Mechanics of Materials 44 (2012) 139–150

Contents lists available at ScienceDirect

Mechanics of Materials

journal homepage: www.elsevier.com/locate/mechmat

Elastic properties of cancellous bone in terms of elastic properties of its mineral and protein phases with application to their osteoporotic degradation

V.A. Lubarda [a,c,*], E.E. Novitskaya [b], J. McKittrick [a,b], S.G. Bodde [b], P.-Y. Chen [b]

[a] Department of Mechanical and Aerospace Engineering, University of California, San Diego, La Jolla, CA 92093-0411, USA
[b] Materials Science Program, University of California, San Diego, La Jolla, CA 92093-0411, USA
[c] Montenegrin Academy of Sciences and Arts, Rista Stijovića 5, 81000 Podgorica, Montenegro

ARTICLE INFO

Article history:
Received 12 December 2010
Received in revised form 1 June 2011
Available online 13 July 2011

Keywords:
Cancellous bone
Cellular solid
Collagen
Elasticity
Mineral
Osteoporosis

ABSTRACT

The elastic modulus of cancellous bone is derived based on the measured elastic properties of separate mineral and protein phases. Adopting the mechanics of cellular solids approach, the moduli of elasticity of cancellous, deproteinated and demineralized bone are expressed in terms of the trabecular moduli of elasticity and the corresponding density ratios using the power law expressions. The Young's modulus of trabeculae of bone are related to the Young's moduli of deproteinated and demineralized trabeculae through a modified mixture rule, which incorporates an appropriate weight function to account for the mineral/protein interaction effects and the departure from the ideal mixture rule. Two expressions for the effective modulus of elasticity of cancellous bone are then derived: one in terms of the moduli of elasticity of mineral and protein trabeculae, and the other in terms of the moduli of elasticity of deproteinated and demineralized cancellous bone. The material parameters are specified from the results of compressive testing of untreated, deproteinated, and demineralized cancellous bovine femur bone. The osteoporotic decrease of the elastic moduli is then analyzed. Two evolution equations are introduced, one for the rate of loss of the mineral content of cancellous bone, and the other for the protein loss. Both losses are associated with the corresponding density and volume changes, for which appropriate equations are proposed. Based on these, and the evolution equations for morphological parameters accounting for the trabecular microarchitecture, the evolution equations are derived for the elastic moduli of deproteinated, demineralized and composite cancellous bone. A particular model of osteoporotic degradation is considered in which it is assumed that the relative ratios of the mineral and protein loss are equal to each other during the progression of osteoporosis.

1. Introduction

Cancellous (trabecular, spongy) bone is a porous inner portion of vertebrae, ribs, skull and the head of the femur, which is surrounded by hard outer layer – cortical (compact) bone. For example, the metaphyses and epiphyses of long bones consist of trabecular compartment surrounded by thin shell of cortical bone; the diaphyses are entirely cortical. Cortical bone predominates in the appendicular skeleton and can resist both tension and compression (thus bending), while cancellous bone is concentrated in the axial skeleton and is structured to resist compression. On the micro-scale, cortical bone consists largely of secondary osteons (10–20 concentric rings of lamellae that surround a central cavity – the Haversian canal, containing

* Corresponding author at: Department of Mechanical and Aerospace Engineering, University of California, San Diego, La Jolla, CA 92093-0411, USA. Tel.: +1 858 534 3169; fax: +1 858 534 5698.
E-mail address: vlubarda@ucsd.edu (V.A. Lubarda).

0167-6636/$ - see front matter © 2011 Elsevier Ltd. All rights reserved.
doi:10.1016/j.mechmat.2011.06.005

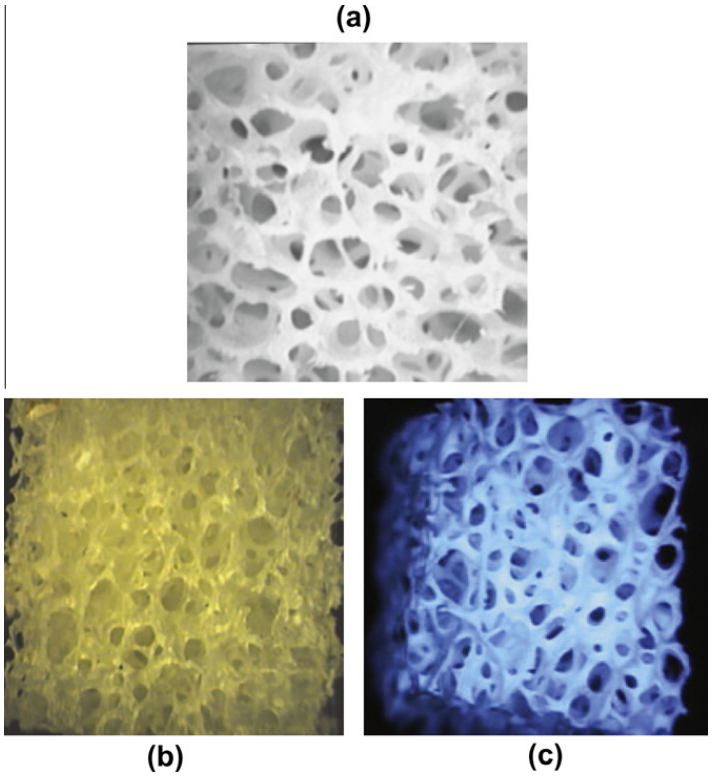

Fig. 1. Photographs of cross-sections (5 × 5 mm) of cancellous bovine femur: (a) control/untreated (UT), (b) demineralized (DM), and (c) deproteinated (DP) bone samples (adopted from Chen et al., 2011). The volumes of the UT, DM, and DP samples are nearly the same, i.e., $V = V_m = V_p$.

one or more blood vessels and nerves). Trabeculae of cancellous bone are composed almost exclusively of lamellar bone arranged in packets (hemiosteons). Cancellous bone is an open cell porous network consisting of rod- and plate-like elements (trabeculae, 50–300 μm thick and up to about 1 mm long), which provide room for blood vessels and marrow, and make the entire bone lighter. While the porosity of cortical bone is in the range of 5–10%, the porosity of cancellous bone is about 40% in the femoral neck, to more than 90% in the elderly spine. Mammalian skeletal bone is made up of around 65 wt.% inorganic matter (mineral phase), 25 wt.% organic matter (dominantly type I collagen), and 10 wt.% water. On a volumetric basis, bone consists of about 33–43 vol.% minerals, 32–44 vol.% organic matter, and 15–25 vol.% water (Gong et al., 1964; Olszta et al., 2007).

Dry cancellous bone can be considered as a composite material consisting of interpenetrating mineral and protein phases. This is confirmed by demineralization and deproteinization processes, which result in stand-alone cellular structures of pure mineral (deproteinated bone) or pure protein (demineralized bone), as shown in Fig. 1. Bone minerals consist of impure hydroxyapatite crystals, $Ca_{10}(PO_4)_6(OH)_2$, with 4–6% of the phosphate groups replaced by carbonate groups, which provides stiffness and strength, while the biopolymer protein phase is composed of type-I collagen, which provides ductility of the bone and its toughness or ability to absorb energy before fracture (Fritsch et al., 2009a,b; Viguet-Carrin et al., 2010). The collagen is also providing a template for mineral deposition, as the mineral crystals are aligned with the collagen fibril axis (Boskey, 2001).

Mechanical properties of cancellous bone are influenced by the trabecular density (fraction of the bone actually occupied by the trabecular bone tissue), the densities of its mineral and protein phases (degree of matrix mineralization and collagen cross-link concentration), their interaction, and the microstructural arrangement of trabecular network (micro-architecture or fabric); Hellmich et al. (2004) and Fritsch and Hellmich (2007).[1] The elastic stiffness and the strength of cancellous bone are nonlinearly related to the apparent bone density (Rice et al., 1988; Keaveny et al., 2001). For example, Marcus and Bouxsein (2008) cite that a 25% decrease in density, associated with 15 years of age-related bone loss, gives rise to 44% decrease of the stiffness of trabecular human bone, with a similar effect on the bone strength. In cancellous bone of the proximal tibia, a decline in apparent density of 25% is associated with a 30–40% reduction in compressive strength and fracture toughness. Microstructural changes of trabecular network due to bone loss, such as thinning or loss of trabecular elements, also exert strong effect on the bone strength. For example, the loss of trabecular connectivity due to the loss of trabecular cross-struts cause a decrease of the buckling strength of isolated trabeculae (Bell et al., 1967), resulting in decrease in strength of the entire bone. In some bones (vertebrae and proximal tibia), the detrimental effect of the decrease of the bone mass on its strength is offset by

[1] There are other factors that may influence mechanical properties of bone. For example, larger crystals may be present in older bone. This increased crystalline size could impair the mechanical properties by permitting earlier crack initiation and decreasing bone ductility (Burr, 2002; Faibish et al., 2006). See also Fantner et al. (2005).

the development of an increased anisotropy of the trabecular structure porosity increases predominantly in the vertical direction, as the horizontally oriented trabeculae thin and disappear faster than vertically oriented trabeculae.[2] This helps the load-carrying capacity along vertical (axial) direction, but is accompanied by the decrease in the load-carrying capacity in horizontal (transverse) directions, which increases the risk of fracture due to nonhabitual, off-axis loading (Ding et al., 2002; Morgan et al., 2008). For example, the ratio of compressive strengths of vertically and horizontally loaded specimens from human lumbar vertebrae increases from approximately 2 at age of 20 to 3.5 at age 80. During this time period, the ash density of vertebral trabecular bone decreases approximately by 50%, with the mechanical properties decrease of as much as 75–90% (Bouxsein, 2008).

The objective of the present paper is to derive the elastic properties of cancellous bone based on the measured elastic properties of isolated mineral and protein phases. After deriving the relationships between the mass densities of individual phases and the composite matrix, the approach from the mechanics of cellular solids is adopted to express the moduli of elasticity of cancellous, deproteinated and demineralized bones in terms of the trabecular moduli of elasticity and the corresponding density ratios using the power law expressions. The Young's modulus of bone's trabeculae are related to the Young's moduli of deproteinated and demineralized trabeculae by a modified mixture rule, in which an appropriate weight function is incorporated to account for the mineral/protein interaction effects and the corresponding departure from the ideal mixture rule. Two alternative expressions for the effective modulus of elasticity of cancellous bone are then derived, one in terms of the moduli of elasticity of mineral and protein trabeculae, and the other in terms of the moduli of elasticity of deproteinated and demineralized bone. It is shown that the modulus of elasticity of cancellous bone is far from being governed by a mixture rule in terms of moduli of elasticity of mineral and protein phases. The presented analysis is applied to cancellous bovine femur bone. The needed material parameters are specified from the results obtained in compressive testing of cancellous samples from untreated, deproteinated, and demineralized femur bone. In the second part of the paper, the osteoporotic deterioration of elastic moduli is studied. Two evolution equations are introduced, one for the rate of loss of the mineral content of cancellous bone, and the other for the protein loss. Both losses are associated with the corresponding density and volume changes, for which appropriate equations are proposed. Based on these, and the evolution equations for morphological parameters accounting for the trabecular microarchitecture, the evolution equations are derived for the elastic moduli of deproteinated, demineralized and composite cancellous bone. An osteoporotic degradation is then considered in which it is assumed that the relative ratios of the mineral and protein loss are equal to each other during the progression of osteoporosis.

2. Volume fractions and density relationships

Consider a representative volume element of cancellous bone whose volume is V.[3] Denoting by V^* the volume of its trabeculae (rods and struts), and by V^o the volume of its hollow portion, we can write $V = V^* + V^o$. Cowin (1999) refers to porosity external to and surrounding the trabeculae as the porosity of the inter-trabecular space. Similarly, if V_p and V_m are the volumes of demineralized (protein) and deproteinated (mineral) phase of the material sample, we can write $V_m = V_m^* + V_m^o$ and $V_p = V_p^* + V_p^o$. Assuming that the bonding interactions between the mineral (m) and protein (p) phase do not appreciably affect the volumes, and since trabecular thinning by demineralization and deproteinization dominantly removes trabecular volume inside the sample (which is an order of magnitude higher that trabecular volume from trabecular elements at the boundary of the sample), it follows that $V = V_m = V_p$ and $V^* = V_m^* + V_p^*$, i.e.,

$$\begin{aligned} &V = V_m = V_m^* + V_m^o, \quad V = V_p = V_p^* + V_p^o, \\ &V = V^* + V^o = V_m^* + V_p^* + V^o, \\ &V_m^o = V^o + V_p^*, \quad V_p^o = V^0 + V_m^*. \end{aligned} \tag{1}$$

The volume fractions of trabeculae and inter-trabecular space are $f^* = V^*/V$ and $f^0 = V^0/V = 1 - f^*$, with similar definitions for f_m^* and f_p^*.

The mass densities (ρ) of cancellous, deproteinated and demineralized bone samples are defined such that

$$\begin{aligned} &m = \rho V = \rho^* V^*, \quad m_m = \rho_m V_m = \rho_m^* V_m^*, \\ &m_p = \rho_p V_p = \rho_p^* V_p^* \end{aligned} \tag{2}$$

with the conservation of mass condition $m = m_m + m_p$. In (2), ρ_m^* is the density of the mineral phase per unit mineral volume within the trabeculae (V_m^*), i.e., $\rho_m^* = m_m/V_m^*$. In contrast, ρ_m is the apparent density of the mineral phase per unit bulk volume (including voided intertrabecular space) of the deproteinated trabecular sample (V_m), i.e., $\rho_m = m_m/V_m$. Similar interpretations apply to densities ρ_p^* and ρ_p of the protein phase. In view of the introduced assumption $V = V_m = V_p$, the conservation of mass yields the additive rule for the cancellous bone density,

$$\rho = \rho_m + \rho_p \tag{3}$$

and the mixture rule for the trabecular density,

$$\rho^* = f_m \rho_m^* + f_p \rho_p^*. \tag{4}$$

The volume fractions of the mineral and protein portions of trabeculae are defined by

$$f_m = V_m^*/V^*, \quad f_p = V_p^*/V^* \quad (f_m + f_p = 1). \tag{5}$$

The corresponding mass ratios are

[2] In accord with Wolffs law, the loaded bone tends to adapt its inner and outer architecture to the environment (loads), so that trabeculae align along stress trajectories to better carry the weight.

[3] The representative volume element (RVE) is small enough to be considered homogeneous in the continuum mechanics sense, but large enough to include sufficiently many trabeculae (or osteons, for cortical bone). We shall later specify the size of RVE in our consideration of cancellous bone to be about $(2\ \text{mm})^3$.

$$c_m = (m_m/m) = (\rho_m/\rho) = f_m(\rho_m^*/\rho^*),$$
$$c_p = (m_p/m) = (\rho_p/\rho) = f_p(\rho_p^*/\rho^*), \tag{6}$$

with $c_m + c_p = 1$. In view of the above definitions and assumptions, the following density relationships can be readily derived

$$(\rho_m/\rho_m^*) = f_m(\rho/\rho^*), \quad (\rho_p/\rho_p^*) = f_p(\rho/\rho^*),$$
$$(\rho/\rho^*) = (\rho_m/\rho_m^*) + \left(\rho_p/\rho_p^*\right). \tag{7}$$

In particular, Eq. (7) specifies the volume fraction of trabeculae, because $(V^*/V) = (\rho/\rho^*)$. The third equation in (7) is obtained by adding the first two. It is also noted that $f_p(\rho_m/\rho_m^*) = f_m(\rho_p/\rho_p^*)$.

Other phase densities could be introduced. For example, the mineral density per unit volume V^* of the trabeculae as a composite (mineral + protein phase) is $\hat{\rho}_m^* = m_m/V^*$. Clearly, $\hat{\rho}_m^* = f_m\rho_m^*$, where $f_m = V_m^*/V^*$ is the mineral volume fraction. Also, if $\rho^* = m/V^*$ is the mass density of the bone per unit volume of trabeculae, then $\rho^* = \hat{\rho}_m^* + \hat{\rho}_p^*$. It may also be recalled that the medical term BMD (bone mineral density) refers to a measure of the mineral density per centimeter square, obtained from X-ray or computed tomography (CT) scan. As such, this measure is used in the medical practice to estimate the strength of bones.

3. Young's moduli of elasticity

Adopting the approach used in the mechanics of cellular solids (Gibson and Ashby, 1997), the effective moduli of elasticity of cancellous bone, and its mineral and protein phase, are related to the moduli of elasticity of the corresponding trabeculae and the density ratios according to

$$E = E^*(\rho/\rho^*)^n, \quad E_m = E_m^*(\rho_m/\rho_m^*)^{n_m}, \quad E_p = E_p^*(\rho_p/\rho_p^*)^{n_p}. \tag{8}$$

These power-law relationships are motivated by the fact that small changes in the density ratios may lead to pronounced changes in the mechanical properties (Carter and Hayes, 1977; Ashby, 1983; Gibson, 1985; Christensen, 1986; Rice et al., 1988; van Rietbergen and Huiskes, 2001). The exponents n, n_m, and n_p depend on the microarchitectural details of trabecular structure (e.g., rod-rod vs. rod-plate like trabeculae).[4] The elastic modulus of such trabeculae (E^*) is not a simple weighted sum of the elastic moduli of pure mineral and pure protein ($E^* \neq f_mE_m^* + f_pE_p^*$), because of interaction effects between the mineral and protein within each trabecula. We thus adopt a modified mixture rule for Young's modulus of trabeculae,

$$E^* = \phi f_mE_m^* + f_pE_p^*, \quad \phi = \phi(f_m). \tag{9}$$

The weight function $\phi = \phi(f_m)$ governs the departure from the ideal mixture rule ($\phi = 1$), and accounts for the effects of interaction between the mineral and protein phase, as well as the differences in micro-porosity or other microarchitectural features of demineralized, deproteinated, and cancellous trabeculae. Lucchinetti (2001) refers to ϕ as an "efficiency or reinforcement" parameter. The individual trabecular moduli E^*, E_m^*, and E_p^* are themselves dependant on the micro-porosity of UT, DP, and DM trabeculae, but this intrinsic (cortical-bone-type) porosity is much smaller than porosity due to intertrabecular space (BV/TV – bone volume/tissue volume), and for simplicity, it is not explicitly included in the analysis in this section, although it will be considered in Section 4, when dealing with osteoporotic degradation of mechanical properties of bone.[5] A simple form $\phi = f_m$ is well-suited to reproduce the experimental data for bovine femur bone, discussed in the next section. When (9) is substituted into (8), the effective modulus of elasticity of cancellous bone (E) can be expressed in terms of the moduli of elasticity of mineral and protein trabeculae (E_m^* and E_p^*), as

$$E = (\phi f_mE_m^* + f_pE_p^*)[(\rho_m/\rho_m^*) + (\rho_p/\rho_p^*)]^n, \tag{10}$$

or, in terms of the moduli of elasticity of mineral and protein phase (E_m and E_p), as

$$E = \phi f_m^{1-n}(\rho_m/\rho_m^*)^{n-n_m}E_m + f_p^{1-n}(\rho_p/\rho_p^*)^{n-n_p}E_p. \tag{11}$$

Clearly, the effective modulus of elasticity of cancellous bone is far from being governed by a mixture rule, i.e., $E \neq f_mE_m + f_pE_p$. There are other more sophisticated tools to estimate the elastic properties of composites, such as those based on the mean field (self-consistent) or microstructural homogenization methods (Nemat-Nasser and Hori, 1999; Zaoui, 2002; Hellmich et al., 2004; Ostoja-Starzewski, 2007; Fritsch et al., 2010; Wang et al., 2009), but we proceed for simplicity with a modified mixture rule (9), leading to (10) and (11).

3.1. Experimental data: bovine femur bone

Sample preparation: Bovine cancellous femur bone samples were obtained from a local butcher. The age of cattle at slaughter was about 18 months. The bone was carefully cleaned to remove any marrow and lipid components, using pressurized stream of compressed air and water. About 100 samples for compression testing (cubes $5 \times 5 \times 5$ mm) were prepared from close locations of the bone in order to minimize variations in density and mineral content. The samples were first roughly cut by handsaw and then by a diamond blade with the surfaces as parallel as possible. Samples were stored in a refrigerator until chemical treatment and testing were performed. The $5 \times 5 \times 5$ mm cubic samples (with mass of about 0.1 g) were the smallest samples we could smoothly cut and test. Smaller cubes, with edge length of about 2 mm

[4] The bone structure of trabeculae is similar to the second (lamellae, lacunae) level of the cortical bone structure. This includes lamellae, lacunae, canaliculi, and cement lines, but generally no vascular channels (like cortical bone). However, lamellae, (2–6) μm thick, are arranged longitudinally within trabecular packets along the trabeculae, while they are arranged concentrically in cortical bone. At the next hierarchial level of structure (below about 0.5 μm), the collagen fibril organization within lamellae, and collagen-mineral structure, are commonly assumed to be the same as for cortical bone.

[5] The bone marrow around trabeculae is very vascularized by embedded capillaries carrying the blood flow and providing oxygen supply, needed for metabolic bone modeling and remodeling. There is a smaller number of vascular structures within trabeculae themselves (Lafage-Proust et al., 2010), which also contribute to their microporosity.

and mass about 5 mg, would still be large enough to contain sufficiently many trabeculae to make them statistically equivalent as representative volume elements. Although we could not experiment with them, they could be considered as the smallest representative element for cancellous bovine femur bone to which our continuum constitutive model applies.[6] More on experimental techniques for bone mechanics, see Turner and Burr (2001).

Demineralization and deproteination process: Bone samples were demineralized (DM) by aging in 0.6 N hydrochloric acid (HCl) at room temperature using the procedures outlined in Toroian et al. (2007) and Chen et al. (2011). Acid solutions were changed daily in order to avoid saturation that can affect the demineralization process. The whole process took about 4 days. The completeness of demineralization was verified by the mineral absence in the solution using the procedure described by Castro-Ceseña et al. (2011). Bone samples were deproteinated (DP) by aging (incubating) in a 2.6 wt.% sodium hypochlorite (NaOCl) solution at 37 °C, following the procedure outlined in Chen et al. (2011) and Chen and McKittrick (in press). The solutions were changed daily, and the whole process took about 7 days.

Compression testing: Three different sets of the samples were prepared: 40 untreated (UT), 30 demineralized (DM) and 30 deproteinated (DP). UT and DP samples were tested in dry condition. DM samples were subjected to a critical point drying procedure before testing in order to avoid an extensive shrinkage. Before compression testing the surfaces of the samples were lubricated by petroleum jelly (vaseline). Compression testing of untreated bone samples was performed on universal testing machine equipped with 30 kN load cell (Instron 3367 Dual Column Testing Systems, Norwood, MA). Compression testing of demineralized and deproteinated bone samples was performed on universal testing machine equipped with 500 N load cell (Instron 3342 Single Column System, Norwood, MA). Compression testing for samples from all three groups was performed at a strain rate of $1 \times 10^{-3}\ \mathrm{s}^{-1}$. An external deflectometer SATEC model I3540 (Epsilon Technology Corp., Jackson, WY) was used in order to measure the small displacement. All samples were loaded until compressive failure.

Experimental data: The reported modulus of elasticity for a single hydroxyapatite crystal is $E_m^* = 114$ GPa (Katz, 1971), while collagen has $E_p^* = 1.3$ GPa (Fung, 1993). The corresponding mass densities are $\rho_m^* = 3.15\ \mathrm{g/cm^3}$ (Heidemann and Riess, 1964) and $\rho_p^* = 1.35\ \mathrm{g/cm^3}$ (Potoczek, 2008). We have tested in our laboratory 20 cortical bone samples from the bovine femur, under dry conditions, and have found that the modulus of elasticity and the mass density were: $E^* = (20 \pm 2)$ GPa and $\rho^* = (2.04 \pm 0.07)\ \mathrm{g/cm^3}$. The modulus of elasticity was determined from the slope of the compressive stress/strain curve. On the other hand, the moduli of elasticity and the mass densities of deproteinated, demineralized, and untreated (control) cancellous samples were:

$$E_m = (295 \pm 80)\ \mathrm{MPa}, \quad \rho_m = (0.48 \pm 0.02)\ \mathrm{g/cm^3},$$
$$E_p = (110 \pm 35)\ \mathrm{MPa}, \quad \rho_p = (0.32 \pm 0.02)\ \mathrm{g/cm^3},$$
$$E = (1.4 \pm 0.3)\ \mathrm{GPa}, \quad \rho = (0.8 \pm 0.03)\ \mathrm{g/cm^3}.$$

The volume ratios of the mineral and protein phases were $f_m = 0.39$ and $f_p = 0.61$, as calculated from (7) with the mean values of the mass densities ρ, ρ_m, ρ_p, and ρ^*. The porosity of the cube specimen, $f^o = (V^o/V) = 1 - f^*$, where $f^* = (V^*/V) = (\rho/\rho^*)$ is the volume fraction of trabeculae, was about 0.6.

The elastic moduli data for E, E_m and E_p was well reproduced from (8) by taking $n_m = 3.15$, $n_p = 1.75$, $n = 2.84$, and $\phi = f_m$. An alternative ϕ that works well is $\phi = \exp[k(f_m - 1)]$, with $k = 3/2$. For example, n was calculated from the expression $n = \ln(E/E^*)/\ln(\rho/\rho^*)$, and similarly for n_m and n_p. It is noted that $E^* \neq f_m E_m^* + f_p E_p^*$ and $E \neq f_m E_m + f_p E_p$, so that the mixture rules are far from being obeyed, particularly for cancellous bones, due to their high cellular porosities. The plots of E^* vs. f_m, according to (9), are shown in Fig. 2. Since the mineral volume fraction in a bovine bone varies generally around 33–43 vol.% mineral, part (b) of Fig. 2 shows the variation of E^* in that range.

4. Osteoporotic degradation of Young's modulus

Osteoporosis is a condition of bone loss and microstructural deterioration of bone tissue, which decreases bone strength and increases skeletal fragility, so that fractures may occur under minor traumas, even those associated with normal daily activities. Progression of osteoporosis is caused by a decline in the bone formation activity relative to the resorption activity (Morita et al., 1994). Since cancellous bone is lighter and more porous than compact bone, it provides more surface area for bone remodeling, it is more metabolically active, and thus more affected by osteoporosis (Ciarallo et al., 2006).[7] Type I osteoporosis signifies a loss of trabecular bone after menopause, caused by the lack of endogenous estrogen, while type II osteoporosis represents a loss of cortical and trabecular bone in men and women as the end result of age-related bone loss, caused by long-term remodeling inefficiency, lack of dietary calcium and vitamin D, and associated mineral absorbtion and handling (Marcus and Bouxsein, 2008). The calcium level in the body, including the amount of calcium in the bones, is regulated by the parathyroid glands through the secretion of parathyroid hormone. Bone degradation due to mineral loss can be determined from measurement of the bone mineral content (BMC), which can be accomplished by quantitative computed tomography, dual-photon absorptiometry, dual X-ray absorptiometry, and ultrasound (Shah et al., 1993). In osteoporosis the likelihood of fracture is 10 to 20 times higher than normal. For example, osteoporosis

[6] The lower hierarchial level would be at the length scale of individual trabeculae, where the study of their individual deformation or fracture could be conducted, e.g., by using micro computed tomography, or high-resolution magnetic resonance (Kaufman and Siffert, 2001; Odgaard, 2001; Viguet-Carrin et al., 2010), and micro finite element modeling of trabecular microarchitecture (van Rietbergen et al., 1995; van Rietbergen and Huiskes, 2001), but such analysis is beyond the scope of the present paper.

[7] The trabecular packets, found in secondary trabecular bone, are products of bone remodeling, which takes place from the outer surface of trabeculae. Osteoclasts first remove bone, and then osteoblasts deposit new bone at the places where the old bone was removed.

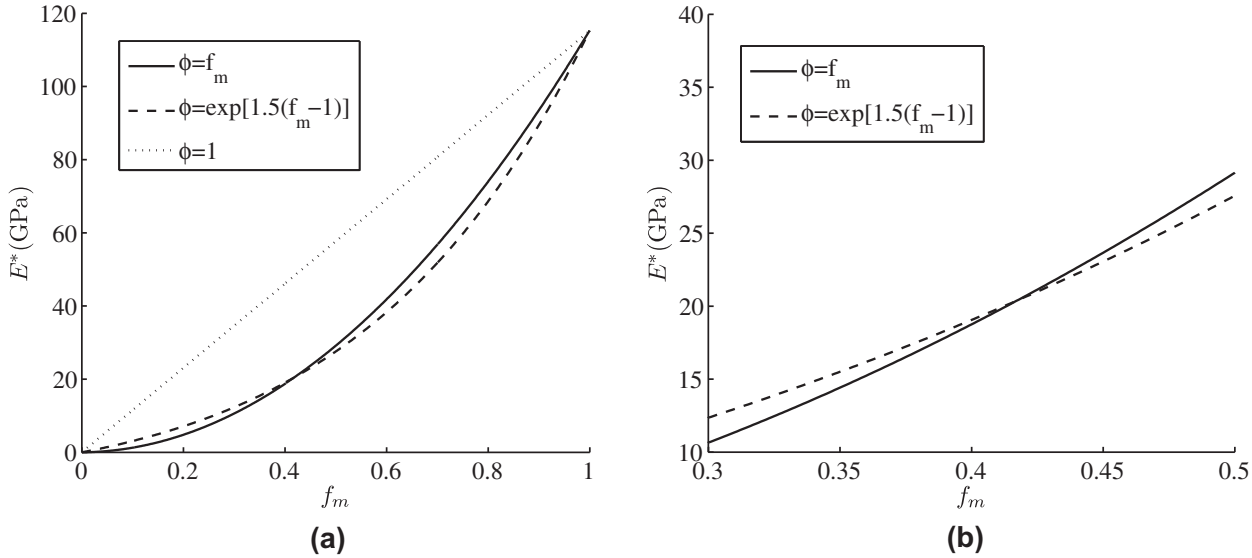

Fig. 2. (a) The variation of the trabecular elastic modulus E^* of cancellous bovine femur with the mineral volume fraction f_m, according to Eq. (9). The pure mineral and protein moduli are $E_m^* = 114$ GPa and $E_p^* = 1.3$ GPa. (b) The variation of E^* in the range around $f_m = 0.4$, characteristic of a bovine femur.

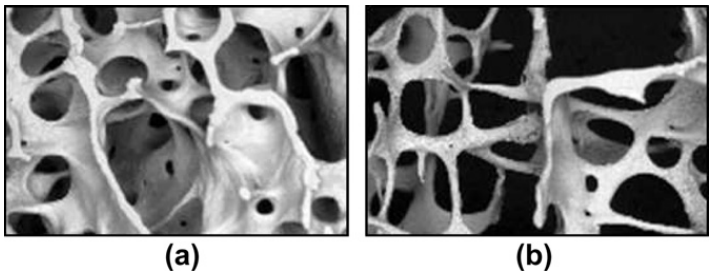

Fig. 3. Trabecular structure of cancellous femur bone: (a) normal, (b) osteoporotic. The osteoporotic bone contains larger holes as a result of the calcium being dissolved and put into the blood stream (from www.brsoc.org.uk/gallery, with permission from Prof. Alan Boyde: (c) a.boyde@qmul.ac.uk).

causes about 1700 bone fractures per day in Europe (according to WHO), the femoral neck fractures being the most frequent (Tellache et al., 2008). It is estimated that osteoporosis is responsible for about 300,000 hip fractures per year in the United States (Ciarallo et al., 2006).

Osteoporosis is a term that describes the loss of calcium from bones due to modification of the remodeling, but in the process of defective remodeling of the bone, in which resorption dominates the deposition, the collagen is lost as well. This results in thinning and resorption of entire individual trabeculae, as shown for an advanced stage of osteoporosis in Fig. 3. The data on the magnitudes of separate mineral and collagen osteoporotic losses are sparse, although there are reports that suggest that their relative concentrations remain approximately constant during osteoporotic bone loss. For example, Burr (2002) reported that there is a decrease in the reducible collagen cross-links in osteoporosis, but without alteration in collagen concentration. The quality of the osteoporotic collagen was reduced by morphological changes in collagen cross-links (Oxlund et al., 1996). The collagen fibers are narrower, loosely packed and more disorganized which, in turn, leads to decreased strength and abnormal mineralization (Bailey et al., 2002). The effect of decreased collagen cross-linking on the biomechanical properties of bone was previously examined by Knott and Bailey (1998).[8]

In our analysis of osteoporotic degradation of elastic bone properties, two evolution equations are proposed, one for the rate of loss of the mineral bone content, and the other for the protein loss, i.e.,

$$\dot{\rho}_m = F_m(\rho_m, \rho_p, \xi_v, t), \quad \dot{\rho}_p = F_p(\rho_m, \rho_p, \xi_v, t) \tag{12}$$

with $\dot{\rho} = \dot{\rho}_m + \dot{\rho}_p$. The physical time is t, and the superposed dot $(\cdot)$ denotes the time rate d/dt. The functions F_m and F_p are the appropriate functions of their indicated arguments. The set of variable ξ_v are the internal state variables, which (together with their own evolution equations) describe the microstructural biochemomechanical changes causing the interactive mineral/protein mass loss. These variables could also account for the specific morphological changes of trabecular architecture, such as thinning or loss/interruptions of trabecular elements, decrease in the trabecular surface available for remodeling, changes in the degree of cross-linking of collagen fibers, etc. (Beaupré

[8] On the other hand, there is a decrease in collagen content with age, which is associated with an increased bone mineralization, but this does cause observable difference in cross-link levels.

et al., 1990; McCalden et al., 1997; Homminga et al., 2003). Although their explicit quantification is a challenging task, left for future investigation, the analysis can proceed based on the general structure (12). Later in the paper, we shall adopt simple phenomenological expressions $\dot{\rho}_m = -r_m t m_m$ and $\dot{\rho}_p = -r_p t m_p$, where r_m and r_m are the bone parameters accounting for the rates of osteoporotic mineral and protein loss of the representative mass element of cancellous bone.[9] Since trabecular volume is dominantly distributed inside of the representative volume sample, the external volume of the very porous bone sample can be taken, to a first approximation, as constant. For example, even the demineralization and deproteinization processes did not appreciably change the external volume V of the samples, as shown in Fig. 1. Thus, the specification of the evolution equations for $\dot{\rho}_m$ and $\dot{\rho}_p$ in (12) also specifies the evolution equations for $\dot{m}_m = V\dot{\rho}_m$ and $\dot{m}_p = V\dot{\rho}_p$.

Since $m_m = \rho_m V = \rho_m^* V_m^*$, it readily follows that

$$\frac{\dot{\rho}_m}{\rho_m} = \frac{\dot{\rho}_m^*}{\rho_m^*} + \frac{\dot{V}_m^*}{V_m^*}, \tag{13}$$

which shows that the (normalized) rate of the mineral loss is associated with the mineral density and volume changes. The experimental data on the magnitudes of these two contributions to the mineral loss is hard to find, and in its absence we introduce a simple partition

$$\frac{\dot{\rho}_m^*}{\rho_m^*} = \psi_m \frac{\dot{\rho}_m}{\rho_m}, \quad \frac{\dot{V}_m^*}{V_m^*} = (1-\psi_m)\frac{\dot{\rho}_m}{\rho_m}, \tag{14}$$

where ψ_m is an appropriate parameter, which may be a constant, or can appropriately vary during progression of osteoporosis ($0 \leqslant \psi_m \leqslant 1$).

Similarly, for the protein phase, we obtain

$$\frac{\dot{\rho}_p}{\rho_p} = \frac{\dot{\rho}_p^*}{\rho_p^*} + \frac{\dot{V}_p^*}{V_p^*}, \tag{15}$$

and

$$\frac{\dot{\rho}_p^*}{\rho_p^*} = \psi_p \frac{\dot{\rho}_p}{\rho_p}, \quad \frac{\dot{V}_p^*}{V_p^*} = (1-\psi_p)\frac{\dot{\rho}_p}{\rho_p}, \tag{16}$$

No further assumptions are needed in the rest of the rate-type analysis presented in this subsection, in which we derive the rates of other geometric or physical properties needed for the subsequent study of elastic moduli degradation, presented in Section 4.1.

First, since $V^* = V_m^* + V_p^*$, by differentiation we obtain

$$\frac{\dot{V}^*}{V^*} = f_m(1-\psi_m)\frac{\dot{\rho}_m}{\rho_m} + f_p(1-\psi_p)\frac{\dot{\rho}_p}{\rho_p}. \tag{17}$$

[9] For the analysis of remodeling of bone in response to changes in long term mechanical loading (adaptive elasticity), see Cowin (1990, 2003) and Currey (2002, 2003). Related references for biomechanical study of soft tissues include Taber (1995), Holzapfel et al. (2000), Humphrey and Rajagopal (2002), Lubarda and Hoger (2002), Lubarda (2004), and Loret and Simoes (2010). The evolving mechanical properties due to microstructural material changes are inherent part of inelastic damage mechanics theories, e.g., Krajcinovic et al. (1993), Lubarda (1994), Krajcinovic (1996), and Davy and Jepsen (2001). See also Thurner et al. (2009).

In view of this, by evaluating the rate of the volume fraction $f_m = V_m^*/V^*$, there follows

$$\dot{f}_m = f_m f_p \left[(1-\psi_m)\frac{\dot{\rho}_m}{\rho_m} - (1-\psi_p)\frac{\dot{\rho}_p}{\rho_p}\right]. \tag{18}$$

Similarly,

$$\dot{f}_p = f_p f_m \left[(1-\psi_p)\frac{\dot{\rho}_p}{\rho_p} - (1-\psi_m)\frac{\dot{\rho}_m}{\rho_m}\right], \tag{19}$$

so that $\dot{f}_m + \dot{f}_p = 0$, as it should be, because $f_m + f_p = 1$ throughout the osteoporotic process (by mere definitions of f_m and f_p).

Second, from $m = \rho V = \rho^* V^*$, we have

$$\frac{\dot{\rho}}{\rho} = \frac{\dot{\rho}^*}{\rho^*} + \frac{\dot{V}^*}{V^*} = \frac{\dot{m}}{m}. \tag{20}$$

Noting that $\dot{\rho} = \dot{\rho}_m + \dot{\rho}_p$, the above can be rewritten as

$$\frac{\dot{\rho}}{\rho} = c_m \frac{\dot{\rho}_m}{\rho_m} + c_p \frac{\dot{\rho}_p}{\rho_p}, \tag{21}$$

where c_m and c_p are the current mass concentrations, as defined in (6), the substitution of (17) and (21) into (20) yields

$$\frac{\dot{\rho}^*}{\rho^*} = [c_m - f_m(1-\psi_m)]\frac{\dot{\rho}_m}{\rho_m} + [c_p - f_p(1-\psi_p)]\frac{\dot{\rho}_p}{\rho_p}. \tag{22}$$

For the analysis in the next section, we need the time rates of three other density ratios ($\rho/\rho^*, \rho_m/\rho_m^*$, and ρ_p/ρ_p^*). They are derived to be

$$\left(\frac{\rho}{\rho^*}\right)^{\cdot} = \frac{\rho}{\rho^*}\left[f_m(1-\psi_m)\frac{\dot{\rho}_m}{\rho_m} + f_p(1-\psi_p)\frac{\dot{\rho}_p}{\rho_p}\right] \tag{23}$$

and

$$\left(\frac{\rho_m}{\rho_m^*}\right)^{\cdot} = \frac{\rho_m}{\rho_m^*}(1-\psi_m)\frac{\dot{\rho}_m}{\rho_m}, \quad \left(\frac{\rho_p}{\rho_p^*}\right)^{\cdot} = \frac{\rho_p}{\rho_p^*}(1-\psi_p)\frac{\dot{\rho}_p}{\rho_p}. \tag{24}$$

4.1. Osteoporotic degradation of Young's moduli

The elastic moduli of pure mineral and protein phases (E_m^* and E_p^*) can be reasonably assumed to depend on the mineral and protein densities (ρ_m^* and ρ_p^*), respectively, i.e., on the microporosity of the individual trabeculae in the deproteinated and demineralized bone samples. Since surface resorption in osteoporosis dominates internal bone deposition, resulting in thinning of the cancellous bone trabeculae, we assume that local (intrinsic) microporosity within individual trabeculae is not rapidly increasing, at least in early stages of osteoporosis, and thus we adopt the simplest linear dependence of the aforementioned elastic moduli on the corresponding densities. This yields the evolution equations

$$\dot{E}_m^* = E_m^* \frac{\dot{\rho}_m^*}{\rho_m^*} = E_m^* \psi_m \frac{\dot{\rho}_m}{\rho_m}, \quad \dot{E}_p^* = E_p^* \frac{\dot{\rho}_p^*}{\rho_p^*} = E_p^* \psi_p \frac{\dot{\rho}_p}{\rho_p}. \tag{25}$$

If $\psi_m = \psi_p = 0$, the elastic moduli E_m^* and E_p^* remain constant during osteoporosis. The evolution equation for the elastic

modulus of the composite (compact) bone of each trabeculae is obtained by differentiating (9). This gives[10]

$$\dot{E}^* = (\phi + \phi' f_m)E_m^* \dot{f}_m + E_p^* \dot{f}_p + \phi f_m \dot{E}_m^* + f_p \dot{E}_p^*, \tag{26}$$

where $\phi' = \mathrm{d}\phi/\mathrm{d}f_m$. If $\dot{E}_m^* = \dot{E}_p^* = 0$, (26) simplifies to

$$\dot{E}^* = \left[(\phi + \phi' f_m)E_m^* - E_p^*\right]\dot{f}_m, \tag{27}$$

with $\dot{f}_m$ give, in terms of density rates $\dot{\rho}_m$ and $\dot{\rho}_p$, by Eq. (18).

We next derive the evolution equations for the elastic moduli of cancellous bone in its deproteinated, demineralized, and untreated state (E_m,E_p, and E). These can be conveniently obtained by differentiating the power law constitutive expressions (8) and by utilizing the previously established expressions for the time rates of the density ratios (23) and (24). The results for the deproteinated and demineralized bones are

$$\frac{\dot{E}_m}{E_m} = \frac{\dot{E}_m^*}{E_m^*} + \dot{n}_m \ln\left(\frac{\rho_m}{\rho_m^*}\right) + n_m(1-\psi_m)\frac{\dot{\rho}_m}{\rho_m}, \tag{28}$$

$$\frac{\dot{E}_p}{E_p} = \frac{\dot{E}_p^*}{E_p^*} + \dot{n}_p \ln\left(\frac{\rho_p}{\rho_p^*}\right) + n_p(1-\psi_p)\frac{\dot{\rho}_p}{\rho_p} \tag{29}$$

and for the untreated bone

$$\frac{\dot{E}}{E} = \frac{\dot{E}^*}{E^*} + \dot{n}\ln\left(\frac{\rho}{\rho^*}\right) + n\left[n_m(1-\psi_m)\frac{\dot{\rho}_m}{\rho_m} + (1-\psi_p)\frac{\dot{\rho}_p}{\rho_p}\right], \tag{30}$$

where $\dot{n}_m$, $\dot{n}_p$, and $\dot{n}$ are the time rates of the morphological parameters which account for the morphological changes (thinning and interruptions) of trabecular structure. Experimental data indicates that smaller values of n_m and n are associated with stiffer trabecular structure, so that n_m and n should be increasing functions of time during progression of osteoporosis. In early stages of osteoporosis, these parameters change only mildly, because trabecular (rod and plate-like) structure is still not significantly altered. In that case their rates can be taken to be equal to zero.

5. A simplified model of osteoporotic degradation

In this section we specialize the analysis by assuming that osteoporosis decreases the bone content such that the ratio m_m/m (and thus also ρ_m/ρ) remains constant. The experimental evidence offers some support for such an assumption (Oxlund et al., 1996; Burr, 2002). Since $m = m_m + m_p$, the constancy of the mineral/bone ratio m_m/m also implies the constancy of the protein/bone ratio m_p/m. Together, they imply that

$$\frac{\dot{m}_m}{m_m} = \frac{\dot{m}_p}{m_p} = \frac{\dot{m}}{m}, \quad \frac{\dot{\rho}_m}{\rho_m} = \frac{\dot{\rho}_p}{\rho_p} = \frac{\dot{\rho}}{\rho}. \tag{31}$$

[10] If f_m and f_p, as well as E_m^* and E_p^*, are already known or determined, Eq. (9) specifies E^* directly, but for the rate-type analysis, particularly when solving the boundary value problems incrementally, the constitutive equations in their rate form are needed.

Furthermore, it readily follows that

$$\frac{\dot{\rho}^*}{\rho^*} = f_m\frac{\dot{\rho}_m^*}{\rho_m^*} + f_p\frac{\dot{\rho}_p^*}{\rho_p^*} = (f_m\psi_m + f_p\psi_p)\frac{\dot{\rho}}{\rho}, \tag{32}$$

$$\dot{f}_m = f_m f_p(\psi_m - \psi_p)\frac{\dot{\rho}}{\rho} = -\dot{f}_p, \tag{33}$$

$$\frac{\dot{V}^*}{V^*} = (1 - f_m\psi_m - f_p\psi_p)\frac{\dot{\rho}}{\rho}. \tag{34}$$

Consistent with the assumed constancy of the mass ratios m_m/m and m_p/m, it is reasonable to also adopt the approximation $\psi_m = \psi_p$ (in the sequel both being denoted by ψ), so that the density changes contribute to the mass changes in the same way for both the mineral and protein phases. In this case, expressions (33) and (34) reduce to

$$\dot{f}_m = \dot{f}_p = 0, \quad \frac{\dot{V}^*}{V^*} = (1-\psi)\frac{\dot{\rho}}{\rho}. \tag{35}$$

The evolution equations for the elastic moduli (25) and (26) accordingly simplify to become

$$\frac{\dot{E}^*}{E^*} = \frac{\dot{E}_m^*}{E_m^*} = \frac{\dot{E}_p^*}{E_p^*} = \psi\frac{\dot{\rho}}{\rho}, \tag{36}$$

while the expressions (28)–(30) reduce to

$$\frac{\dot{E}_m}{E_m} = \dot{n}_m \ln\left(\frac{\rho_m}{\rho_m^*}\right) + [\psi + n_m(1-\psi)]\frac{\dot{\rho}}{\rho}, \tag{37}$$

$$\frac{\dot{E}_p}{E_p} = \dot{n}_p \ln\left(\frac{\rho_p}{\rho_p^*}\right) + [\psi + n_p(1-\psi)]\frac{\dot{\rho}}{\rho}, \tag{38}$$

$$\frac{\dot{E}}{E} = \dot{n}\ln\left(\frac{\rho}{\rho^*}\right) + [\psi + n(1-\psi)]\frac{\dot{\rho}}{\rho}. \tag{39}$$

5.1. Numerical evaluations

The bone mass at a given time of adult life is the peak bone mass attained at skeletal maturity minus the subsequently lost bone mass. Traditional radiographic techniques cannot distinguish osteoporosis until it is severe (Marcus and Bouxsein, 2008), which implies that the rate of osteoporotic bone loss is initially very low, perhaps even zero. Accordingly, we propose that the time rate of bone density $\dot{\rho}$ is proportional to the product of the current density ρ, providing an exponential decay, and the time t, providing a vanishing rate of bone loss at the onset of osteoporosis ($t = 0$). If needed to better reproduce clinical observations, or provide more accurate prognosis, the power t^k, with an appropriately adjusted value of k, can be used in place of t. Thus, we propose simple evolution equations for the mineral, protein, and composite bone content

$$\frac{\dot{\rho}_m}{\rho_m} = \frac{\dot{\rho}_p}{\rho_p} = \frac{\dot{\rho}}{\rho} = -rt, \tag{40}$$

where r is the coefficient with the dimension $(\text{time})^{-2}$, which accounts for the rate of the mass resorption. If r is

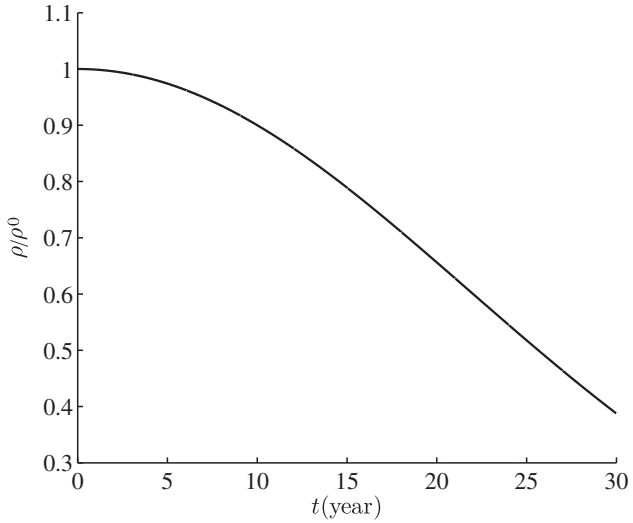

Fig. 4. The time variation of the bone density ratio (ρ/ρ^o) during 30 years of progression of osteoporosis, according to Eq. (40), with the rate coefficient $r = 2.107 \times 10^{-3}\,(\text{year})^{-2}$.

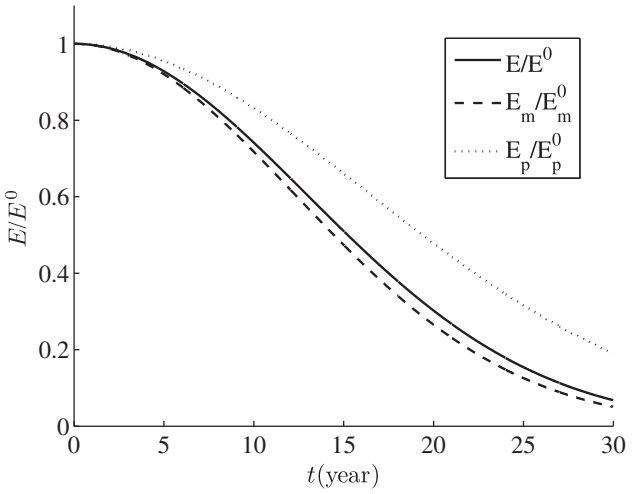

Fig. 5. The time variations of the elastic moduli ratios E/E^0, E_m/E_m^0 and E_p/E_p^0 during their osteoporotic degradation, according to (45)–(47), corresponding to constant values of the morphological parameters $n = 2.84$, $n_m = 3.15$ and $n_p = 1.75$, and with the rate coefficient $r = 2.107 \times 10^{-3}\,(\text{year})^{-2}$.

assumed to be constant, (40) can be integrated analytically to obtain

$$\rho_m = \rho_m^0 \exp(-rt^2/2), \quad \rho_p = \rho_p^0 \exp(-rt^2/2),$$
$$\rho = \rho^0 \exp(-rt^2/2), \tag{41}$$

where ρ_m^0, ρ_p^0, and ρ^0 are the corresponding densities at the onset of osteoporosis. Furthermore, we shall take for the simplicity of numerical evaluations that $\psi_m = \psi_p = 0$, which means that the entire mass loss takes place by the reduction of volume (thinning and interruptions of trabeculae), without density changes, i.e., $\dot\rho^* = \dot\rho_m^* = \dot\rho_p^* = 0$. The volume fractions f_m and f_p are constant, while $\dot V^*/V^* = -rt$.

The elastic moduli (36) and (37) of trabeculae vanish,[11] $\dot E^* = \dot E_m^* = \dot E_p^* = 0$, while the expressions (37)–(39) for the elastic moduli of cancellous bone reduce to

$$\frac{\dot E_m}{E_m} = \dot n_m \ln\left(\frac{\rho_m}{\rho_m^*}\right) + n_m \frac{\dot\rho}{\rho}, \tag{42}$$

$$\frac{\dot E_p}{E_p} = \dot n_p \ln\left(\frac{\rho_p}{\rho_p^*}\right) + n_p \frac{\dot\rho}{\rho}, \tag{43}$$

$$\frac{\dot E}{E} = \dot n \ln\left(\frac{\rho}{\rho^*}\right) + n \frac{\dot\rho}{\rho}. \tag{44}$$

Their integrated forms, given by (7), can be expressed as

$$E_m = E_m^0 \exp(-rn_m t^2/2), \quad E_m^0 = E_m^*(\rho_m^0/\rho_m^*)^{n_m}, \tag{45}$$

$$E_p = E_p^0 \exp(-rn_p t^2/2), \quad E_p^0 = E_p^*(\rho_p^0/\rho_p^*)^{n_p}, \tag{46}$$

$$E = E^0 \exp(-rnt^2/2), \quad E^0 = E^*(\rho^0/\rho^*)^n. \tag{47}$$

For example, if osteoporosis decreases the bone content by 10% in 10 years, from (41) the coefficient r is equal to $2.107 \times 10^{-3}(\text{year})^{-2}$. The corresponding time variation of the mass or density ratios, such that ρ/ρ^0, determined from (41), is shown in Fig. 4. The predicted bone density decrease after 15 years is 21.1%; after 20 years it is 34.4%, and after 25 years it is 48.2%. Fig. 5 shows the osteoporotic degradation of the latter moduli, calculated from (45)–(47), if the morphological parameters[12] $n_m = 3.15$, $n_p = 1.75$, and $n = 2.84$ did not change with time. For example, after 10 years these moduli decrease to $E_m = 0.718E_m^0$, $E_p = 0.832E_p^0$, and $E = 0.742E^0$, while after 20 years they are $E_m = 0.266E_m^0$, $E_p = 0.479E_p^0$, and $E = 0.303E^0$. The different magnitudes of the decrease is due to different trabecular microarchitectures of deproteinated, demineralized and untreated cancellous bone specimens, and their different microarchitecture, accounted for by different values of the morphological parameters n_m, n_p and n in (45)–(47).

If needed to better match the observed data (e.g., to increase or decrease the rate of osteoporotic deterioration of Young's moduli), the time dependent expressions for the morphological parameters n_m, n_p and n can be included in the analysis. For example, by adopting the rate expression $\dot n = -0.012t^{1/2}$, i.e., $n = 2.84 - 0.008t^{3/2}$, so that $n = 2.84$ and $\dot n = 0$ at $t = 0$, the modulus of elasticity E decreases after 10 years to $E = 0.762E^0$, and after 20 years to $E = 0.409E^0$ (dashed curve in Fig. 6). The corresponding decreased values of the morphological parameter n were 2.587 and 2.125. Even less pronounced degradation of elastic modulus is predicted by adopting a cubic expression $n = 2.84 - 0.0036t^2 + 0.00006t^3$. In this case, the bone's modulus of elasticity decreases after 10 years to

[11] This means that, although the amount of bone is reduced by aging and osteoporosis, the bone of remaining trabeculae is histologically normal, so that the moduli E_m^*, E_p^* and E^* remain unchanged.

[12] These values were determined in Section 3.1 from the density and elastic moduli values of bovine femur bone. The elastic coefficients of human femur are nearly the same as of bovine femur bone (Bronzino, 2000, Table 18-2, p. 18-6). Human femoral neck samples, obtained from hip replacement surgeries, were tested by Ciarallo et al. (2006). Comparable to the bovine samples, they found that the compressive strength and the modulus of the human samples are correlated, and are within the range of published values for the human femoral neck (Martens et al., 1983).

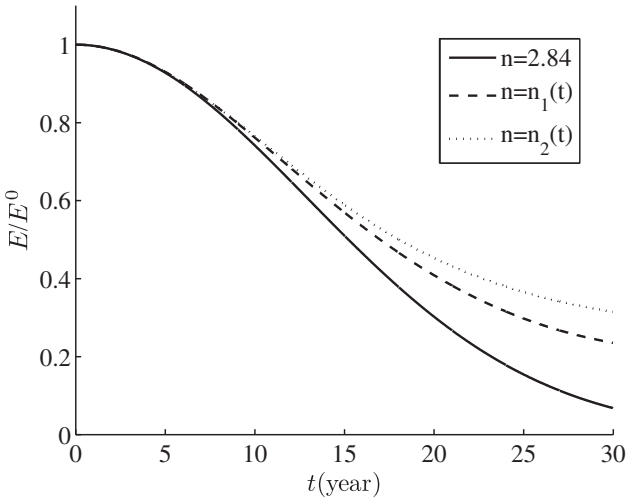

Fig. 6. The time variation of the elastic moduli ratio of cancellous bone E/E^0 during its osteoporotic degradation, according to (47), in the case when the morphological parameter $n = 2.84$ is constant, or equal to time dependent function $n_1(t) = 2.84 - 0.008t^{1.5}$ or $n_2(t) = 2.84 - 0.0036t^2 + 0.00006t^3$.

$E = 0.766E^0$, and after 20 years to $E = 0.453E^0$ (dotted curve in Fig. 6). The corresponding values of the morphological parameter n were 2.541 and 1.881. Regarding experimental data for human cancellous bone, we found in the literature that for the vertebral trabecular bone specimens, a decrease in bone tissue of about 9% over 10 years causes a decrease of the elastic modulus of about 15% in the axial direction (along spine), and about 16% in transverse direction (Bouxsein, 2008, Table 23-1, p. 605).

6. Conclusions and discussion

We have presented in this paper an analysis of the Young's modulus of cancellous bone based on that of the isolated mineral and protein phases. The Young's modulus of cancellous trabeculae is related to the Young's moduli of deproteinated and demineralized trabeculae by a modified mixture rule, in which an appropriate weight function is introduced to account for the mineral/protein interaction effects and the corresponding departure from the ideal mixture rule. Adopting the approach from the mechanics of cellular solids, two alternative expressions for the modulus of elasticity of cancellous bone are derived: one in terms of the moduli of elasticity of mineral and protein trabeculae, and the other in terms of the moduli of elasticity of deproteinated and demineralized bone. The presented analysis is applied to cancellous bovine femur bone. The material parameters are determined experimentally by compression testing of untreated, deproteinated, and demineralized cancellous bovine femur bone. The osteoporotic decrease of the elastic moduli is then analyzed. The evolution equations are introduced for the rate of loss of the mineral content of cancellous bone, and for the protein loss. Both losses are associated with the corresponding density and volume changes, for which appropriate equations are proposed. Based on these, and the evolution equations for morphological parameters accounting for the trabecular microarchitecture, the evolution equations are derived for the elastic moduli of deproteinated, demineralized and composite cancellous bone. A particular model of osteoporotic degradation is considered in which it is assumed that the relative ratios of the mineral and protein loss are equal to each other during the progression of osteoporosis. The rate parameter is adjusted so that the bone content decreases by 10% in 10 years, which yields the decrease of the modulus of elasticity by about 25%. The straightforward adjustment of the morphological parameters of trabecular microarchitecture can modify (slow) the rate of the elastic moduli degradation if needed to better match the experimental data.

The extension of the presented work is needed to encompass the determination of other elastic properties, the Poisson ratio and the shear modulus of cancellous bone, in terms of the elastic properties of its mineral and protein phases, as well as the effect of stress on the osteoporotic degradation of elastic properties. Decreased physical activity of osteoporotic patients or differences in intensity of load transferred to osteoporotic bone vs. healthy bone exert their effects on progression of osteoporosis (van Rietbergen et al., 2003; Gefen et al., 2008). Furthermore, the development of elastic anisotropy of cancellous bones during osteoporosis is an essential aspect of the analysis. This requires the description of the trabecular fabric changes (trabecular size and shape changes, trabecular loss of connectivity), dependent on biochemical factors causing the mineral and collagen decay, sustained mechanical loads, and the type of cancellous bone (e.g., Fyhrie and Carter, 1986; Carter et al., 1987; Cowin et al., 1992; Sugita et al., 1999; Keaveny, 2001; Hart, 2001; Hing, 2004). For example, trabeculae in vertebrae are mostly rod-like, while in the metaphyses and epiphyses of long bones the trabecular structure consists of a more balanced mixture of the rod- and plate-like trabeculae. These different cellular structures will degrade differently by the progression of resorption cavities, resulting in differences in the degree and the nature of the induced elastic anisotropy. Morita et al. (1994) observed the highest progression rate of osteoporosis in rod/rod trabecular structure; the next highest rate was in plate/bar-like structure, while the plate/plate-like trabecular structure was the least sensitive. The degree of initial elastic anisotropy also varies among different types of cancellous bones. While cancellous bone from the lumbar vertebrae are approximately transversely isotropic, that from the iliac crest and central femoral head are nearly isotropic. This is a consequence of functional differences between different bones: the vertebrae are weight-bearing, whereas the iliac crest is not (Dempster, 2000). The biomechanics study of such aspects of bone behavior is challenging from theoretical, computational, and experimental points of view.

Acknowledgment

Research support from the National Science Foundation, Division of Materials Research, Biomaterials Program (Grant DMR 0510138) and Ceramics Program (Grant DMR 1006931) is gratefully acknowledged. V.A.L. acknowledges

research support from the Montenegrin Academy of Sciences and Arts. We also thank four referees for their helpful criticism and suggestions.

References

Ashby, M.F., 1983. The mechanical properties of cellular solids. Metal. Mater. Trans. A 14, 1755–1769.

Bailey, A.J., Sims, T.J., Knott, L., 2002. Phenotypic expression of osteoblast collagen in osteoarthritic bone: Production of type I homotrimer. Int. J. Biochem. Cell Biol. 34, 176–182.

Beaupré, G.S., Orr, T.E., Carter, D.R., 1990. An approach for time-dependent modeling and remodeling – theoretical development. J. Orthop. Res. 8, 651–661.

Bell, G.H., Dunbar, O., Beck, J.S., 1967. Variations in strength of vertebrae with age and their relation to osteoporosis. Calc. Tiss. Res. 1, 75–86.

Boskey, A.L., 2001. Bone mineralization. In: Cowin, S.C. (Ed.), Bone Mechanics Handbook. CRC Press, Boca Raton, FL, pp. 5-1–5-33 (Chapter 5).

Bouxsein, M.L., 2008. Biomechanics of age-related fractures. In: Marcus, R., Feldman, D., Nelson, D., Rosen, C.J. (Eds.), Osteoporosis, 3rd ed. Elsevier, Inc., pp. 601–621 (Chapter 23).

Bronzino, J.D. (Ed.), 2000. The Biomedical Engineering Handbook, vol. 1. CRC Press, Boca Raton, FL.

Burr, D.B., 2002. Bone material properties and mineral matrix contributions to fracture risk or age in women and men. J. Musculoskel. Neuron Interact. 2, 201–204.

Carter, D.R., Hayes, W.C., 1977. The compressive behavior of bone as a two-phase porous structure. J. Bone Joint Surg. Am. 59, 954–962.

Carter, D.R., Fyhrie, D.P., Whalen, R.T., 1987. Trabecular bone density and loading history: Regulation of connective tissue biology by mechanical energy. J. Biomech. 20, 785–794.

Castro-Ceseña, A.B., Novitskaya, E.E., Chen, P.-Y., Hirata, G.A., McKittrick, J., 2011. Kinetic studies of bone demineralization at different HCl concentrations and temperatures. Mater. Sci. Eng. C 31, 523–530.

Chen, P.-Y., McKittrick, J., in press. Compressive mechanical properties of demineralized and deproteinized cancellous bone. J. Mech. Behav. Biomed. Mater.

Chen, P.-Y., Toroian, D., Price, P.A., McKittrick, J., 2011. Minerals form a continuum phase in mature cancellous bone. Calcif. Tiss. Inter. 88, 351–361.

Christensen, R.M., 1986. Mechanics of low density materials. J. Mech. Phys. Solids 34, 563–578.

Ciarallo, A., Barralet, J., Tanzer, M., Kremer, R., 2006. An approach to compare the quality of cancellous bone from the femoral necks of healthy and osteoporotic patients through compression testing and microcomputed tomography imaging. McGill J. Med. 9, 102–107.

Cowin, S.C., 1990. Structural adaptation of bones. Appl. Mech. Rev. 43, S126–S133.

Cowin, S.C., 1999. Bone poroelasticity. J. Biomech. 32, 217–238.

Cowin, S.C., 2003. Adaptive elasticity: A review and critique of a bone tissue adaptation model. Eng. Trans. 51, 1–79.

Cowin, S.C., Sadegh, A.M., Luo, G.M., 1992. An evolutionary Wolff's law for trabecular architecture. J. Biomech. Eng. 114, 129–136.

Currey, J.D., 2002. Bones: Structures and Mechanics. Princeton University Press, Princeton.

Currey, J.D., 2003. The many adaptations of bone. J. Biomech. 36, 1487–1495.

Davy, D.T., Jepsen, K.J., 2001. Bone damage mechanics. In: Cowin, S.C. (Ed.), Bone Mechanics Handbook. CRC Press, Boca Raton, FL, pp. 18-1–18-25 (Chapter 16).

Dempster, D.W., 2000. The contribution of trabecular architecture to cancellous bone quality. J. Bone Mineral Res. 15, 20–23.

Ding, M., Odgaard, A., Linde, F., Hvid, I., 2002. Age-related variations in the microstructure of human tibial cancellous bone. J. Orthop. Res. 20, 615–621.

Faibish, D., Ott, S.M., Boskey, A.L., 2006. Mineral changes in osteoporosis: A review. Clin. Orthop. Relat. Res. 443, 28–38.

Fantner, G.E., Hassenkam, T., Kindt, J.H., Weaver, J.C., Birkedal, H., Pechenik, L., Cutroni, J.A., Cidade, G.A., Stuky, G.D., Morse, D.E., Hansma, P.K., 2005. Sacrificial bonds and hidden length dissipate energy as mineralized fibrils separate during bone fracture. Nature Mater. 4, 612–616.

Fritsch, A., Hellmich, C., 2007. 'Universal' microstructural patterns in cortical and trabecular, extracellular and exrtravascular bone materials: Micromechanics-based prediction of anisotropic elasticity. J. Theor. Biol. 244, 597–620.

Fritsch, A., Dormieux, L., Hellmich, C., Sanahuja, J., 2009a. Mechanical behavior of hydroxyapatite biomaterials: An experimentally validated micromechanical model for elasticity and strength. J. Biomed. Mater. Res. Part A 88, 149–161.

Fritsch, A., Hellmich, C., Dormieux, L., 2009b. Ductile sliding between mineral crystals followed by rupture of collagen crosslinks: Experimentally supported micromechanical explanation of bone strength. J. Theor. Biol. 260, 230–252.

Fritsch, A., Hellmich, C., Dormieux, L., 2010. The role of disc-type crystal shape for micromechanical predictions of elasticity and strength of hydroxyapatite biomaterials. Phil. Trans. R. Soc. A 368, 1913–1935.

Fung, Y.C., 1993. Biomechanics: Mechanical Properties of Living Tissues. Springer–Verlag, New York.

Fyhrie, D.P., Carter, D.R., 1986. A unifying principle relating stress to trabecular bone morphology. J. Orth. Res. 4, 304–317.

Gefen, A., Portnoy, S., Diamant, I., 2008. Inhomogeneity of tissue-level strain distributions in individual trabeculae: Mathematical model studies of normal and osteoporosis cases. Med. Eng. Phys. 30, 624–630.

Gibson, L.J., 1985. The mechanical behavior of cancellous bone. J. Biomech. 18, 317–328.

Gibson, L.J., Ashby, M.F., 1997. Cellular Solids: Structure and Properties, 2nd ed. Cambridge Univ. Press, Cambridge, England.

Gong, J.K., Arnold, J.S., Cohn, S.H., 1964. Composition of trabecular and cortical bone. Anat. Rec. 149, 325–332.

Hart, R.T., 2001. Bone modeling and remodeling: Theories and computation. In: Cowin, S.C. (Ed.), Bone Mechanics Handbook. CRC Press, Boca Raton, FL, pp. 31-1–31-42 (Chapter 31).

Heidemann, E., Riess, W., 1964. Die Veranderungen Des Kollagens Bei Entwasserung Mit Aceton + Die Konsequenzen Dieser Veranderung Für Die Kollagenstruktur. Hoppe-Seyler's Z. Physiol. Chem. 337, 101.

Hellmich, C., Barthélémy, J.-F., Dormieux, L., 2004. Mineral-collagen interactions in elasticity of bone ultrastructure - a continuum micromechanics approach. Eur. J. Mech. A/Solids 23, 783–810.

Hing, K.A., 2004. Bone repair in the twenty-first century: Biology, chemistry or engineering. Phil. Trans. R. Soc. Lond. A. 362, 2821–2850.

Holzapfel, G.A., Gasser, T.C., Ogden, R.W., 2000. A new constitutive framework for arterial wall mechanics and a comparative study of material models. J. Elast. 61, 1–48.

Homminga, J., McCreadie, B.R., Weinans, H., Huiskes, R., 2003. The dependence of the elastic properties of osteoporotic cancellous bone on volume fraction and fabric. J. Biomech. 36, 1461–1467.

Humphrey, J.D., Rajagopal, K.R., 2002. A constrained mixture model for growth and remodeling of soft tissues. Math. Models Methods Appl. Sci. 12, 407–430.

Katz, J.L., 1971. Hard tissue as a composite material. I: Bounds on the elastic behavior. J. Biomech. 4, 244–473.

Kaufman, J.J., Siffert, R.S., 2001. Strength of trabecular bone. In: Cowin, S.C. (Ed.), Bone Mechanics Handbook. CRC Press, Boca Raton, FL, pp. 34-1–34-25 (Chapter 34).

Keaveny, T.M., 2001. Strength of trabecular bone. In: Cowin, S.C. (Ed.), Bone Mechanics Handbook. CRC Press, Boca Raton, FL, pp. 16-1–16-42 (Chapter 16).

Keaveny, T.M., Morgan, E.F., Niebur, G.L., Yeh, O.C., 2001. Biomechanics of trabecular bone. Annu. Rev. Biomed. Eng. 3, 307–333.

Knott, L., Bailey, A.J., 1998. Collagen cross-links in mineralizing tissues. Review of their chemistry, function, and clinical relevance. Bone 22, 181–187.

Krajcinovic, D., 1996. Damage Mechanics. North-Holland, Amsterdam.

Krajcinovic, D., Lubarda, V., Sumarac, D., 1993. Fundamental aspects of the brittle cooperative phenomena. Mech. Mater. 15, 99–115.

Lafage-Proust, M.-H., Prisby, R., Roche, B., Vico, L., 2010. Bone vascularization and remodeling. Joint Bone Spine 77, 521–524.

Loret, B., Simoes, F.M.F., 2010. Elastic-growing tissues: A growth rate law that satisfies the dissipation inequality. Mech. Mater. 42, 782–796.

Lubarda, V.A., 1994. An analysis of large-strain damage elastoplasticity. Int. J. Solids Struct. 31, 2951–2964.

Lubarda, V.A., 2004. Constitutive theories based on the multiplicative decomposition of deformation gradient: Thermoelasticity, elastoplasticity and biomechanics. Appl. Mech. Rev. 57, 95–108.

Lubarda, V.A., Hoger, A., 2002. On the mechanics of solids with a growing mass. Int. J. Solids Struct. 39, 4627–4664.

Lucchinetti, E., 2001. Composite models of bone properties. In: Cowin, S.C. (Ed.), Bone Mechanics Handbook. CRC Press, Boca Raton, FL, pp. 12-1–12-19 (Chapter 12).

Marcus, R., Bouxsein, M., 2008. The nature of osteoporosis. In: Marcus, R., Feldman, D., Nelson, D., Rosen, C.J. (Eds.), Osteoporosis, 3rd ed. Elsevier, Inc, pp. 27–36 (Chapter 2).

Martens, M., Van Audekercke, R., Delport, P., De Meester, P., Mulier, J.C., 1983. The mechanical characteristics of cancellous bone at the upper femoral region. J. Biomech. 16, 971–983.

McCalden, R.W., McGeough, J.A., Court-Brown, C.M., 1997. Age-related changes in the compressive strength of cancellous bone: The relative importance of changes in density and trabecular architecture. J. Bone Joint Surg. 79, 421–427.

Morgan, E.F., Barnes, G.L., Einhorn, T.A., 2008. The bone organ system: Form and function. In: Marcus, R., Feldman, D., Nelson, D., Rosen, C.J. (Eds.), Osteoporosis, 3rd ed. Elsevier, Inc, pp. 3–25 (Chapter 1).

Morita, M., Ebihara, A., Itoman, M., Sasada, T., 1994. Progression of osteoporosis in cancellous bone depending on trabecular structure. Ann. Biomed. Eng. 22, 532–539.

Nemat-Nasser, S., Hori, M., 1999. Micromechanics: Overall Properties of Heterogeneous Materials, 2nd ed. North-Holland, Amsterdam.

Odgaard, A., 2001. Quantification of cancellous bone architecture. In: Cowin, S.C. (Ed.), Bone Mechanics Handbook. CRC Press, Boca Raton, FL, pp. 14-1–14-19 (Chapter 14).

Olszta, M.J., Cheng, X., Jee, S.S., Kumar, R., Kim, Y.-Y., Kaufman, M.J., Douglas, E.P., Gower, L.B., 2007. Bone structure and formation: A new perspective. Mater. Sci. Eng. R 58, 77–116.

Ostoja-Starzewski, M., 2007. Microstructural Randomness and Scaling in Mechanics of Materials. Chapman and Hall/CRC Press, Boca Raton, FL.

Oxlund, K., Mosekilde, L., Ørtoft, G., 1996. Reduced concentration of collagen reducible cross human trabecular bone with respect to age and osteoporosis. Bone 19, 479–494.

Potoczek, M., 2008. Hydroxyapatite foams produced by gelcasting using agarose. Mater. Lett. 62, 1055–1057.

Rice, J.C., Cowin, S.C., Bowman, J.A., 1988. On the dependence of the elasticity and strength of cancellous bone on apparent density. J. Biomech. 21, 155–168.

Shah, K.M., Gob, J., Bose, K., 1993. The relationship between femoral neck strength, bone mineral content and fracture fixation strength: An in vitro study. Osteoporosis Int. (Suppl. 1), S51–S53.

Sugita, H., Oka, M., Toguchida, J., Nakamura, T., Ueo, T., Hayami, T., 1999. Anisotropy of osteoporotic cancellous bone. Bone 24, 513–516.

Taber, L.A., 1995. Biomechanics of growth, remodeling, and morphogenesis. Appl. Mech. Rev. 48, 487–545.

Tellache, M., Rixrath, E., Chabrand, P., Hochard, C., Pithioux, M., Wendling-Mansuy, S., 2008. Numerical simulation of an osteoporotic femur: Before and after total hip arthroplasty. Eur. J. Comput. Mech. 17, 785–793.

Thurner, P.J., Erickson, B., Turner, P., Jungmann, R., Lelujian, J., Proctor, A., Weaver, J.C., Schitter, G., Morse, D.E., Hansma, P.K., 2009. The effect of NaF in vitro on the mechanical and material properties of trabecular and cortical bone. Adv. Mater. 21, 451–457.

Toroian, D., Lim, J.L., Price, P.A., 2007. The size exclusion characteristics of type I collagen: Implications for the role of non-collagenous bone constituents in mineralization. J. Biol. Chem. 282, 22437–22484.

Turner, C.H., Burr, D.B., 2001. Experimental techniques for bone mechanics. In: Cowin, S.C. (Ed.), Bone Mechanics Handbook. CRC Press, Boca Raton, FL, pp. 7-1–7-35 (Chapter 7).

van Rietbergen, B., Huiskes, R., 2001. Elastic constants of cancellous bone. In: Cowin, S.C. (Ed.), Bone Mechanics Handbook. CRC Press, Boca Raton, FL, pp. 15-1–7-24 (Chapter 15).

van Rietbergen, B., Weinans, H., Huiskes, R., Odgaard, A., 1995. A new method to determine trabecular bone elastic properties and loading using micromechanical finite-element models. J. Biomech. 28, 69–81.

van Rietbergen, B., Huiskes, R., Eckstein, F., Ruegsegger, P., 2003. Trabecular bone tissue strains in the healthy and osteoporotic human femur. J. Bone Miner. Res. 18, 1781–1788.

Viguet-Carrin, S., Follet, H., Gineyts, E., Roux, J.P., Munoz, F., Chapurlat, R., Delmas, P.D., Bouxsein, M.L., 2010. Association between collagen cross-links and trabecular microarchitecture properties of human vertebral bone. Bone 46, 342–347.

Wang, C., Feng, L., Jasiuk, I., 2009. Scale and boundary conditions effects on the apparent elastic moduli of trabecular bone modeled as a periodic cellular solid. J. Biomech. Eng. 131. Art. no. 121008-1-11.

Zaoui, A., 2002. Continuum micromechanics: Survey. J. Eng. Mech. (ASCE) 128, 808–816.